DOI:10.1093/jnci/dju184
First published online August 8, 2014

ARTICLE

Investigation of Schwann Cells at Neoplastic Cell Sites Before the Onset of Cancer Invasion

Ihsan Ekin Demir*, Alexandra Boldis*, Paulo L. Pfitzinger, Steffen Teller, Eva Brunner, Natascha Klose, Timo Kehl, Matthias Maak, Marina Lesina, Melanie Laschinger, Klaus-Peter Janssen, Hana Algül, Helmut Friess, Güralp O. Ceyhan

*Authors contributed equally to this work.

Manuscript received November 5, 2013; revised May 20, 2014; accepted May 27, 2014.

Correspondence to: Ihsan Ekin Demir, MD, Department of Surgery, Klinikum rechts der Isar, Technische Universität München, Ismaninger Str. 22, D-81675 München, Germany (e-mail: ekin.demir@tum.de).

Background In neural invasion (NI), cancer cells are classically assumed to actively invade nerves and to cause local recurrence and pain. However, the opposite possibility, that nerves may reach cancer cells even in their preinvasive stage and thereby promote cancer spread, has not yet been genuinely considered. The present study analyzes the reaction of Schwann cells of peripheral nerves to carcinogenesis in pancreatic cancer and colon cancer.

Methods Two novel 3D migration and Schwann cell outgrowth assays were developed to monitor the timing and the specificity of Schwann cell migration and cancer invasion toward peripheral neurons through digital-time-lapse microscopy and after blockade of nerve growth factor (NGF) signalling via siRNA or a small-molecule inhibitor of the $p75^{NTR}$ receptor. The frequency and emergence of the Schwann cell markers Sox10, S100, ALDH1L1, and glial-fibrillary-acidic-protein (GFAP) around cancer precursor lesions were studied in human and conditional murine pancreatic and colon cancer specimens using multiple immunolabeling.

Results Schwann cells migrated toward pancreatic and colon cancer cells, but not toward benign cells, before the onset of cancer migration toward peripheral neurons. This chemoattraction was inhibited after blockade of $p75^{NTR}$-signaling on Schwann and pancreatic cancer cells. Schwann cells were specifically detected around murine and human pancreatic intraepithelial neoplasias (PanINs) (mean percent of murine PanINs surrounded by Schwann cells = 78.9%, 95% CI = 70.9 to 86.8%, and mean percent of human PanINs surrounded by Schwann cells = 52.5%, 95% CI = 14.7 to 90.4%; human: n = 44, murine: n = 14) and intestinal adenomas (mean percent of murine adenomas surrounded by Schwann cells = 64.2%, 95% CI = 28.6 to 99.8%, and mean percent of human adenomas surrounded by Schwann cells = 17.2%, 95% CI = -126.9 to 161.4; human: n = 36, murine: n = 12). The Schwann cell presence in this premalignant stage was associated with the frequency of NI in the malignant phase.

Conclusions Schwann cells have particular and specific affinity to cancer cells. Emergence of Schwann cells in the premalignant phase of pancreatic and colon cancer implies that, in contrast with the traditional assumption, nerves—and not cancer cells—migrate first during NI.

JNCI J Natl Cancer Inst (2014) 106(8): dju184 doi:10.1093/jnci/dju184

Neural invasion (NI) is one of the most common paths of cancer spread in several solid malignant tumors, including pancreas, prostate, colon, and squamous cell tumors of the head and neck (1). In pancreatic cancer, cancer cells already invade prevertebral nerve plexus even in the early T1 tumor stages (2,3). This observation suggests that malignant tumors, even when very small in size, have strong affinity to nerves (4) and gain early access to nerves for cancer dissemination. However, the possibility that nerves with their inherent cells (eg, glia cells and neurons) may react to carcinogenesis at its earliest steps and be attracted to malignant and/or transformed cells even before cancer invasion has not yet been investigated.

The most prevalent cell type in peripheral nerves is the neural glia, ie, Schwann cells. In the present study, we hypothesized that Schwann cells of peripheral nerves may be attracted to cancer cells before the onset of actual cancer invasion and thereby provide the first access to nerves for cancer cells during tumor progression.

Methods

Cell Lines and Cell Culture

The following cell lines were purchased from American Type Culture Collection/ATCC and cultured according to the supplier's recommendations: human PCa cell line SU86.86, human CCa cell lines DLD-1 and SW620, human glioblastoma cell line LN229, human fibroblast cell line BJ. The human T3M4 PCa cell line was a kind gift by Dr. Metzgar (Durham, North Carolina). Primary rat

pancreatic stellate cells/PaStC were isolated from three- to eight-day-old newborn Wistar rats by the outgrowth method, as described previously and cultured in Dulbecco's Modified Eagle's Medium/DMEM:Ham's F12 (1:1) medium supplemented with 20% fetal calf serum/FCS, 100 U/mL penicillin, and 100 µg/mL streptomycin at 37°C in a humid atmosphere, saturated with 5% CO_2 (5). Human pancreatic ductal epithelial cells (HPDE) were a kind gift from Professor M.S. Tsao of the Ontario Cancer Institute (Toronto, Canada) (6,7), the Mode-K mouse colon epithelial cell line (8) from Professor D. Haller, Nutrition and Food Research Centre, TU Munich, and the mouse colorectal cancer cell line CMT-93 from Professor Holzmann, Department of Surgery, TU Munich. The primary dorsal root ganglia/DRG neurons were freshly isolated from newborn Wistar rats, as described before (9). To achieve the best possible neuronal growth, usage of mitotic inhibitors or additional neurotrophic factors was avoided in DRG cultures. Human Schwann cells/hSC and rat Schwann cells/rSC were derived from human or rat spinal nerves as primary cells and can be cultured up to a maximum of 10 passages (ScienCell Research Laboratories, Carlsbad, CA). hSC and rSC were grown in complete Schwann cell medium containing 5% FCS and Schwann cell growth supplement cocktail (ScienCell, Carlsbad, CA). The purity of the cultures was assessed through multiple immunolabeling experiments using glial (GFAP, Sox10) and fibroblast (Vimentin, Desmin) markers.

Three-Dimensional (3D) Neural Migration Assay

The recently demonstrated 3D migration assay and digital time lapse microscopy were utilized to investigate the migratory behaviour of Schwann cells and cancer cells (9). This assay allows the simultaneous confrontation of multiple cell types and analysis of their: 1) morphological reactions to confrontation with each cell type, 2) targeted migratory behavior, and 3) heterotypic cell–cell interactions upon establishment of physical contact. Here, 10^5 cells of each type and dorsal root ganglia (DRG) neurons isolated from three newborn rat lumbar DRGs were suspended in an extracellular matrix/ECM gel drop (E1270, from Engelbreth-Holm-Swarm [EHS] mouse sarcoma, Sigma-Aldrich, Munich, Germany), placed at an exact 1-mm distance to each other and connected via an ECM "bridge" for generation of a chemoattractive gradient (Figure 1). In order to exclude unspecific cellular interactions, the cell suspensions were connected to an additional cell-free ECM gel. After polymerization of ECM suspensions and bridges, a 1:1 mixture of Neurobasal medium (supplemented with 100 U/mL penicillin and 100 µg/mL streptomycin, 2% B-27 and 0.5 mM L-Glutamin) and the medium of each cancer or non-neoplastic cell type was applied to the assay. At 72 hours after seeding of the assay, ECM gels containing each cell type were excised from the culture dish and incubated in Hank's Balanced Salt Solution (HBSS), supplied with collagenase type II (1 mg/ml, Worthington Biochemical, Lakewood, NJ) for 15 minutes to allow the dissociation of the cells from the ECM gel and subsequently lysed in radioimmunoprecipitation (RIPA) buffer containing Complete, a protease inhibitor cocktail (Roche, Penzberg, Germany).

3-D Schwann Cell Outgrowth and Migration Assay

In order to test the specificity of tumor-directed migration of Schwann cells, a novel 3-D Schwann cell migration assay was established. For this purpose, a 5-mm segment of the left or right sciatic nerve of newborn Wistar rats was placed at a 1-cm distance away from a 25-µl ECM gel suspension containing pancreatic cancer cells. To enable neural invasion by pancreatic cancer cells, a thin ECM bridge was pipetted between the pancreatic cancer cell suspension and the sciatic nerve. In order to ensure the maximum distance of the exposed Schwann cells at the both ends of the excised nerve segment, it was placed vertically to the ECM bridge. The outgrowth of Schwann cells was video documented daily and stopped at day seven of coculture by fixation with 4% paraformaldehyde (Carl Roth GmbH, Karlsruhe, Germany) and analyzed after subsequent immunofluorescence labeling.

Conditional Mouse Models of Pancreatic and Colon Carcinogenesis

Mutant Kras in combination with mutated or absent trp53 is known to result in metastatic pancreatic ductal adenocarcinoma in mice, reflecting all major features of human pancreatic cancer (10,11). Therefore, the LSL-KrasG12D knock-in (12), p48-cre (13) and $Trp53^{fl/fl}$ (14) strains were interbred to obtain LSL-KrasG12D;$Trp53^{fl/fl}$;p48-cre (termed KP) mice. Mutant LSL-$Kras^{G12D}$;p48-cre (termed KC) mice are known to develop the putative precursor of pancreatic cancer, ie, pancreatic intraepithelial neoplasia (PanIN) lesions and to exhibit pancreatic cancer at around one year of age. Several small intestinal and colon adenomas are known to emerge in mice carrying a mutated APC allele (APC+/1638N, termed APC). When these mice are interbred with mice expressing a common mutated Kras ($Kras^{V12G}$) under the control of the mouse villin promoter (APC+/1638N;$Kras^{V12G}$, termed APCK), these mice develop colon cancer (CCa).

Mice at 8 to 12 weeks of age were killed in order to obtain whole pancreas, small intestine, and colon, which were either formalin fixed and paraffin embedded, or submerged in Tissue-Tek (Sakura Finetek, Torrance, CA, USA) and snap-frozen in liquid nitrogen for cryosectioning and further histopathological analysis. In the histopathology, the number of precursor or overt cancer cell sites on a given section were counted and proportioned to the total number of precursor and cancer cell clusters per section and expressed as percent. All procedures were approved by the governmental commission for animal protection of the Government of Upper Bavaria (Regierung Oberbayern, 2005/01).

Human PCa, Chronic Pancreatitis, Colon Adenoma and CCa Tissues

PCa and chronic pancreatitis (CP) tissue samples from the pancreatic head were collected from patients following tumor resection (patient characteristics: Supplementary Table 1, available online). Human colon adenomas were obtained from patients undergoing routine screening colonoscopy, and the CCa specimens from patients with cancer of the ascending or descending colon (Supplementary Table 1, available online). Tissue samples were processed as described previously (2,15). All patients were informed, and written consent was obtained for tissue collection. The study was approved by the ethics committee of the Technische Universität München (Munich, Germany).

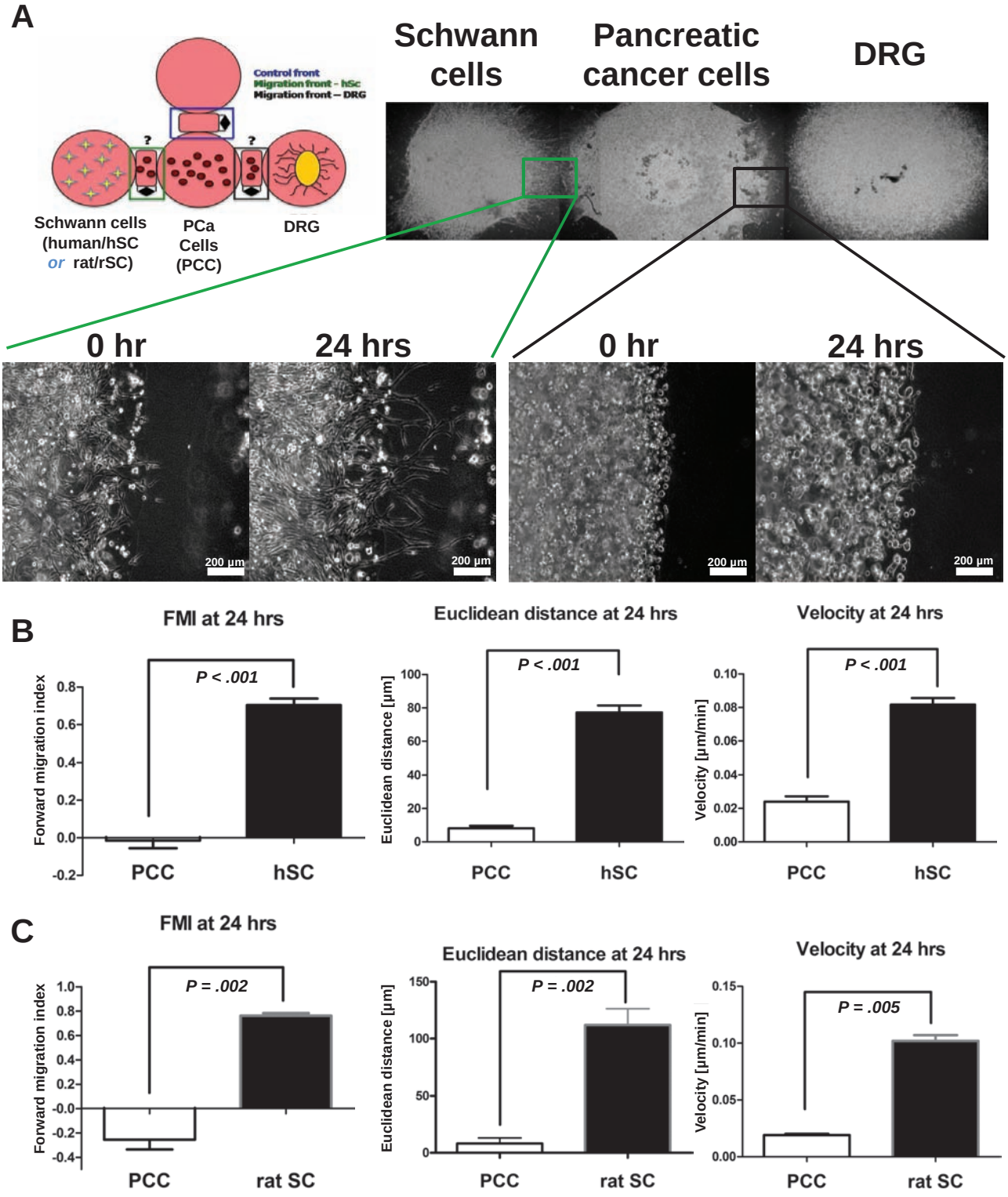

Figure 1. Chemoattraction of primary human Schwann cells to pancreatic cancer (PCa) cells via NGF/p75^{NTR}. **A)** Pancreatic cancer cells (PCC) were simultaneously confronted with dorsal root ganglia/DRG neurons on one side and with human Schwann cells (hSC) on the other in the 3D-neural-migration assay (**green box**: Schwann cells migration front; **black box**: pancreatic cancer migration front) and tracked using digital time-lapse microscopy. **B)** Average forward migration index/FMI of hSC (toward PCC) when compared to the FMI of PCC (toward neurons) at 24 hours of cocultivation. Please also see the FMI of PCC toward DRG at 48 hours of cocultivation in Supplementary Figure 1 **(available online)**. **C)** FMI, linear (Euclidean) distance of migration and migration velocity of rat Schwann cells (rSC, toward human PCC) when compared with the migration features of PCC (toward rat neurons). All comparisons were carried out using the Mann Whitney U test. The results were created from three independent experiments. All statistical tests were two-sided.

Statistical Analysis

Two-group analyses were performed using the Mann–Whitney-U test or unpaired *t*-test, and more than two-group analyses were conducted using the Kruskal–Wallis or one-way analysis of variance test, followed by Dunn's multiple comparison or Bonferroni's multiple comparison test. Results are expressed as mean followed by 95% confidence interval (CI). All tests were two-sided, and a *P* value of < .05 was considered to indicate statistical significance.

Results

Schwann Cell Chemoattraction to Pancreatic Cancer Cells

To test our hypothesis, we first used a three-dimensional/3D migration-assay in which pancreatic cancer cells were simultaneously confronted with primary human or rat Schwann cells on one side and with rat dorsal root ganglia/DRG neurons on the other side (Figure 1) (9). This coculture system revealed a previously unexpected finding in terms of the reaction of Schwann cells to cancer. Here, after 24 hours of cocultivation, before pancreatic cancer cells even started with their migration toward neurons, Schwann cells had already formed a stream of cells migrating toward pancreatic cancer cells (Figure 1A). Comparative quantification of this cancer-directed Schwann cell migration revealed that the whole human Schwann cell population exhibited a highly targeted cellular migration toward the different pancreatic cancer cells (T3M4, SU86.86), as evidenced by their higher forward migration index (FMI) (FMI = 0.54, 95% CI = 0.47 to 0.63, and FMI = 0.37, 95% CI = 0.31 to 0.43, respectively, $P < .001$) when compared to pancreatic cancer cells (FMI = –0.01, 95% CI = –0.1 to 0.07 for both pancreatic cancer cells; Figure 1B; Supplementary Figure 1, A and B, available online). Rat Schwann cells were used in additional experiments to exclude species-specific chemoattraction of glia to human cancer cells. Similar to human Schwann cells, also rat Schwann cells exhibited a very early and highly targeted migration to human T3M4 pancreatic cancer cells (FMI = 0.76, 95% CI = 0.71 to 0.81, $P = .002$) than cancer cells to neurons (FMI = -0.26, 95% CI = –0.46 to –0.05) (Figure 1C). As primary, nontransformed cells, this targeted migration of Schwann cells was not due to a "faster migration" or longer linear distance covered toward pancreatic cancer cells, since the velocity and migration distance of Schwann cells did not differ between their migration and empty-gel-facing front (Supplementary Figure 1, available online). It was only after 48 hours of cocultivation when pancreatic cancer cells started their specific migration toward DRG (Supplementary Figure 1, available online).

This cancer-chemoattraction of Schwann cells necessitated further validation. For this purpose, a novel in vitro Schwann cell outgrowth assay was established, which enabled the confrontation of pancreatic cancer cells directly with nerves—and not neurons, as so far performed in available NI models (4,9,16,17). Indeed, pancreatic cancer cells are rather surrounded by nerves and their fibers in the pancreatic tissue, as opposed to neuronal cell bodies, which reside outside the pancreas, eg, in DRG and other extrinsic ganglia. Hence, for a migration of Schwann cells toward cancer cells to occur, Schwann cells must grow out of the nerves where they reside. In this assay, explanted newborn rat sciatic nerves were placed perpendicular to the connecting bridge between the nerve and the pancreatic cancer cells, thereby assuring the maximum distance between the exposed Schwann cells at the site of nerve transsection and pancreatic cancer cells. Forty-eight hours after transsection and the start of outgrowth of Schwann cells out of the sciatic nerve, Schwann cells diverted their initial vertical outgrowth direction and made a sharp "U turn" toward the pancreatic cancer cells, before these had even left their original ECM gel (Figure 2, A and B), and sought contact with the tip of the pancreatic cancer cell-migration front. Remarkably, there were nearly no Schwann cells at all that grew in the opposite direction with no pancreatic cancer cells (Figure 2, A and B). Quantification of the Schwann cell outgrowth toward pancreatic cancer cells revealed a highly specific Schwann cell migration toward cancer cells, as evidenced by higher FMI (to SU86.86: FMI = 0.53, 95% CI = 0.35 to 0.72, and to T3M4: FMI = 0.43, 95% CI = 0.28 to 0.59, $P = .004$ for both cell lines) at their cancer-targeting front than at their nontargeting front (back front: FMI = 0.01, 95% CI = –0.52 to 0.54, and FMI = 0.12, 95% CI = –0.11 to 0.35; Figure 2C). Migration of potentially contaminating fibroblasts was excluded through double-immunolabeling with GFAP and the fibroblast marker Vimentin, which confirmed the migrating cells as glial cells (Figure 2D).

Specificity of Schwann Cell Migration Toward Malignant—and Not Benign—Cells

To test the specificity of cancer-chemoattraction of Schwann cells, pancreatic cancer cells and other malignant cells from the gastrointestinal tract, ie, human colon cancer cells (DLD-1, SW620), and human glioblastoma cells (LN229) as a nervous-system–related, nongastrointestinal malignancy, were simultaneously cocultured (Supplementary Figure 2, available online). Furthermore, benign cells like human fibroblasts/BJ or pancreatic stellate cells/PAStC were used as additional controls. To have pancreas- or colon-derived epithelial controls, human pancreatic ductal epithelial cells (HPDE) and the colon epithelial cell line (Mode-K) were used in additional assays (Supplementary Figure 4, available online). Here, Schwann cells did not demonstrate any targeted movement toward any of these benign cell types and also no chemoatttraction toward the LN229 glioblastoma cell line. However, Schwann cells indeed migrated toward DLD-1 and SW620 human colon cancer cells with a statistically significantly greater FMI (DLD-1: FMI = 0.54, 95% CI = 0.49 to 0.59, and SW620: FMI = 0.5, 95% CI = 0.42 to 0.58, $P < .05$ for both cell lines) than toward control suspension (FMI = 0.37, 95% CI = 0.32 to 0.42, and 0.24, 95% CI = 0.16 to 0.32, respectively; Supplementary Figures 2 and 3, available online). This Schwann cell migration did not reach the noticeable extent toward the two different pancreatic cancer cells (FMI = 0.6, 95% CI = 0.55 to 0.63, and FMI = 0.77, 95% CI = 0.69 to 0.85, respectively, $P < .05$ for both cell lines; Supplementary Figures 2 and 3, available online). Based on these observations, Schwann cells as primary, non-neoplastic cells that normally reside within peripheral nerves can obviously get activated and chemoattracted by cancer cells and "take the first step" to get in contact with them.

Regulation of the Chemoattraction Between Human Schwann Cells, Pancreatic Cancer Cells and Neurons by the NGF-TrkA-p75^{NTR} Axis

Molecular factors mediating this newly identified targeted migration of Schwann cells toward cancer cells are not known. Here,

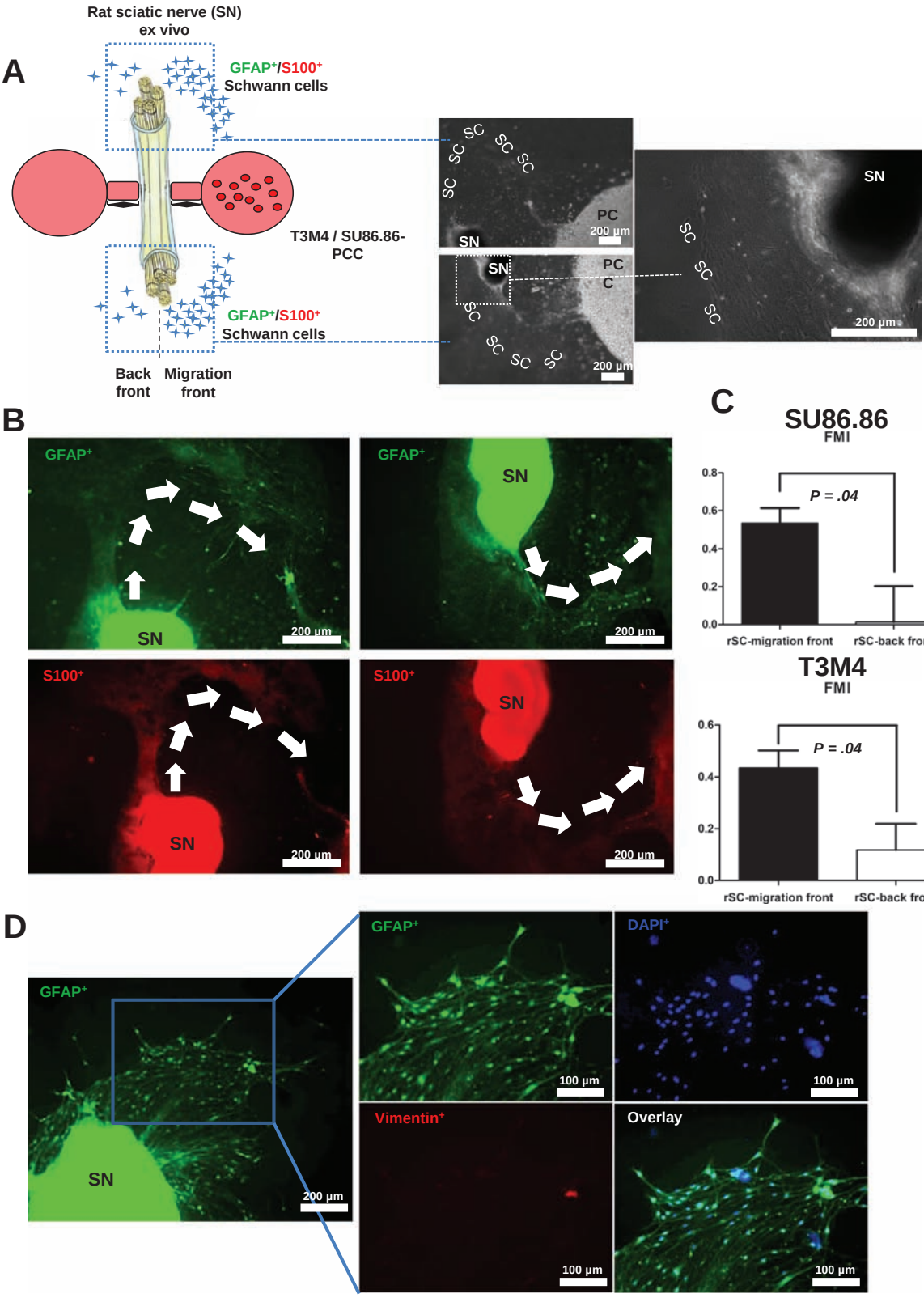

Figure 2. The targeted outgrowth of Schwann cells out of explanted nerves toward pancreatic cancer cells: a novel 3D Schwann cell-outgrowth assay. **A)** To investigate the carcinotropic potential of Schwann cells (SC), ex vivo rat sciatic nerves (SN) were placed perpendicular to a connecting extracellular matrix/ECM bridge to T3M4 and SU86.86 pancreatic cancer cells (PCC) and tracked for rat Schwann cell (rSC) outgrowth. **B)** The diversion of the initially vertical outgrowth direction of S100/GFAP-double-immunoreactive toward pancreatic cancer cells, indicated by the **arrows**. **C)** Quantification and comparison of rSC forward migration index (FMI) toward T3M4 or SU86.86 PCC in comparison to the control extracellular matrix gel suspension (ie, back front). **D)** Exclusion of fibroblast contamination via double immunolabeling with the glial marker GFAP, the fibroblast marker Vimentin, and concomintant nuclear labelling. All comparisons were carried out using the Mann-Whitney U test. The results were created from three independent experiments. All statistical tests were two-sided.

we compared the levels of nerve growth factor (NGF), its high-affinity receptor TrkA, and its low-affinity receptor $p75^{NTR}$ in Schwann cells that had been cocultivated with pancreatic cancer cells. The choice for these molecules was based on the increasing number of reports on the elevated expression of this trio in pancreatic cancer and their recently demonstrated contribution to neuroplasticity in pancreatic cancer (18,19). The cocultivation of these cells resulted in increased NGF levels in both pancreatic cancer cells and Schwann cells. Particularly, Schwann cells in dual coculture with pancreatic cancer cells demonstrated greater (1.4-fold, 95% CI = 1.0 to 1.8-fold, $P = .04$) intracellular levels of NGF than control Schwann cells in monoculture, with a similar tendency for Schwann cells in triple-coculture with pancreatic cancer cells and DRG neurons (mean densitometry value = 2.1-fold, 95% CI = 0.73-±.3.47-fold) (Figure 3A). Furthermore, the dual or triple coculture was associated with a 2.2-fold (95% CI = 0.24 to 4.16) and 1.8-fold (95% CI = 0.62 to 2.98) elevation of intracellular NGF levels in pancreatic cancer cells as well (Figure 3A).

In order to elucidate the impact of the two NGF isoforms, ie, beta-NGF and pro-NGF, on the chemoattraction of Schwann cells to pancreatic cancer cells, human Schwann cells were incubated with increasing doses of beta-NGF and pro-NGF. Here, increasing doses of particularly beta-NGF ($P = .01$ for T3M4 and $P = .009$ for SU86.86 at 50 ng/ml beta-NGF), but to a lesser extent also of pro-NGF, augmented Schwann cell transmigration toward two different types of pancreatic cancer cell lines (Figure 3B).

Increased NGF levels in Schwann cells cocultured with pancreatic cancer cells raised the question on the expression levels of NGF, pro-NGF, $p75^{NTR}$, and of the alternative $p75^{NTR}$ ligand brain-derived neurotrophic factor (BDNF) in human and murine pancreatic tissues. In human pancreatic cancer tissues, the average mRNA expression levels for $p75^{NTR}$ were higher than in normal human pancreas ($P = .002$), with a similar tendency for the NGF expression levels (Figure 3C). There was no difference in the mRNA levels of BDNF in normal human vs pancreatic cancer tissues. In murine tissue, there was a similar, progressive increase in $p75^{NTR}$ expression from wild-type normal pancreas over 12-week old KC mice, which contained the PanIN precursor lesions, to KP mice with overt pancreatic cancer ($P = .04$, Figure 3D). Similarly, the levels of NGF mRNA were prominently greater in KP tumors than in KC ($P = .02$) or wild-type pancreas ($P = .03$, Figure 3D). In contrast with human tissues, there was a continuous increase in BDNF levels, from wild type over KC to KP pancreatic tissue ($P = .007$, Figure 3D). To detect pro-NGF in the pancreatic tissue, we performed immunoblotting with human normal pancreas and pancreatic cancer tissues. Here, pro-NGF was detected in its 53kDa isoform (20), and there was a prominent increase in the detected amounts of proNGF in human pancreatic cancer when compared with normal pancreas (Supplementary Figure 5D, available online).

Pretreatment of Schwann cells with a small-molecule inhibitor of TrkA and $p75^{NTR}$ (Ro 08-2750, Tocris Bioscience), which in a dose-dependent manner either only blocked $p75^{NTR}$ (at 500 nM and 5 µM) or both receptors at the higher dose (50 µM), resulted in attenuation of Schwann cells migration toward pancreatic cancer cells, as evidenced by the decrease in their FMI ($P = .01$ for 500 nM and $P < .001$ for 5 µM, Figure 3E). Similarly, when $p75^{NTR}$ expression was silenced in human Schwann cells via specific siRNA, the targeted migration and FMI of Schwann cells toward pancreatic cancer cells was prominently decreased (FMI of Control-siRNA: 0.53, 95% CI = 0.41 to 0.66; FMI of $p75^{NTR}$-siRNA: 0.35, 95% CI = 0.31 to 0.38, $P = .04$, Figure 3F). Strikingly, pretreatment of pancreatic cancer cells led to diminished invasion of DRG neurons by pancreatic cancer cells (Supplementary Figure 5C, available online), suggesting a crucial role for the NGF-$p75^{NTR}$ ligand-receptor pair in NI in pancreatic cancer.

Identification of Schwann Cells Around Conditional Murine and Human Pancreatic Cancer and Colon Cancer Precursor Lesions

Schwann cells can be easily identified by immunolabeling with traditional Schwann cells markers like S100, glial-fibrillary-acidic-protein/GFAP, and the glial fate acquisition marker Sox10 (21). In a conditional murine pancreatic cancer model (p48-Cre/LSL-$Kras^{G12D}$; KC model [22]), which exhibits the typical precursor lesions of pancreatic cancer, ie, the PanIN, double immunolabeling with the glial makers GFAP and S100 revealed the presence of a specific Schwann-cell niche in murine neoplastic tissue. Here, Schwann cells were specifically encountered around the PanIN lesions of the KC model, at their basolateral aspect (Figure 4A). Astonishingly, Schwann cells were completely absent in the normal neighboring pancreatic parenchyma (Figure 4A), pointing to an "on-off-phenomenon" between normal and neoplastic pancreatic tissue. In a more aggressive murine pancreatic cancer model (p48-Cre;LSL-$Kras^{G12D}$;$Trp53^{-/-}$, KP model, [23]), Schwann cells were similarly found around ductal cancer lesions (Figure 4B). Similar to the murine models, in human pancreatic tissues (eg, from patients with chronic pancreatitis) demonstrating PanIN lesions of varying severity, Schwann cells were equally present around such precursor lesions (Figure 4C). Interestingly, some of these cells lacked GFAP but were immunoreactive for the Schwann cell identity marker Sox10 (Figure 4C). In human pancreatic cancer, these cells were again preserved around cancer cell clusters and at sites of NI (Figure 4D). Moreover, in human pancreatic cancer, enlarged stromal nerves seemed to lack clearly identifiable perineural sheaths, and to harbour S100-GFAP double-immunoreactive cells in their direct surroundings, which seemed to lack any continuous connection to these nerves (Figure 4D). In order to exclude the detection of neural crest-derived, non-glial cells by these markers, we additionally performed double immunolabeling with GFAP and the highly specific astrocyte marker ALDH1L1 (24) in murine and human pancreas. Also here, double-immunolabeled glial cells were detected in the same niches, ie, around murine and human PanIN lesion, as with the other markers (Supplementary Figure 6, available online).

In order to test the specificity of Schwann cell emergence around pancreatic cancer precursor lesions, the distribution of Schwann cells in human and murine colon cancer specimens were investigated (Figure 5). Similar to pancreatic cancer, Schwann cells were specifically encountered within the dysplastic cell clusters in the $Apc^{1638N/+}$ intestinal adenoma model (termed APC [25], Figure 5A) and along nerve fibers dispersed among cancer cells in murine colon cancer ($Apc^{1638N/+}$;KrasV12G, termed APCK) (26) (Figure 5B). On the other hand, in both human colon adenomas

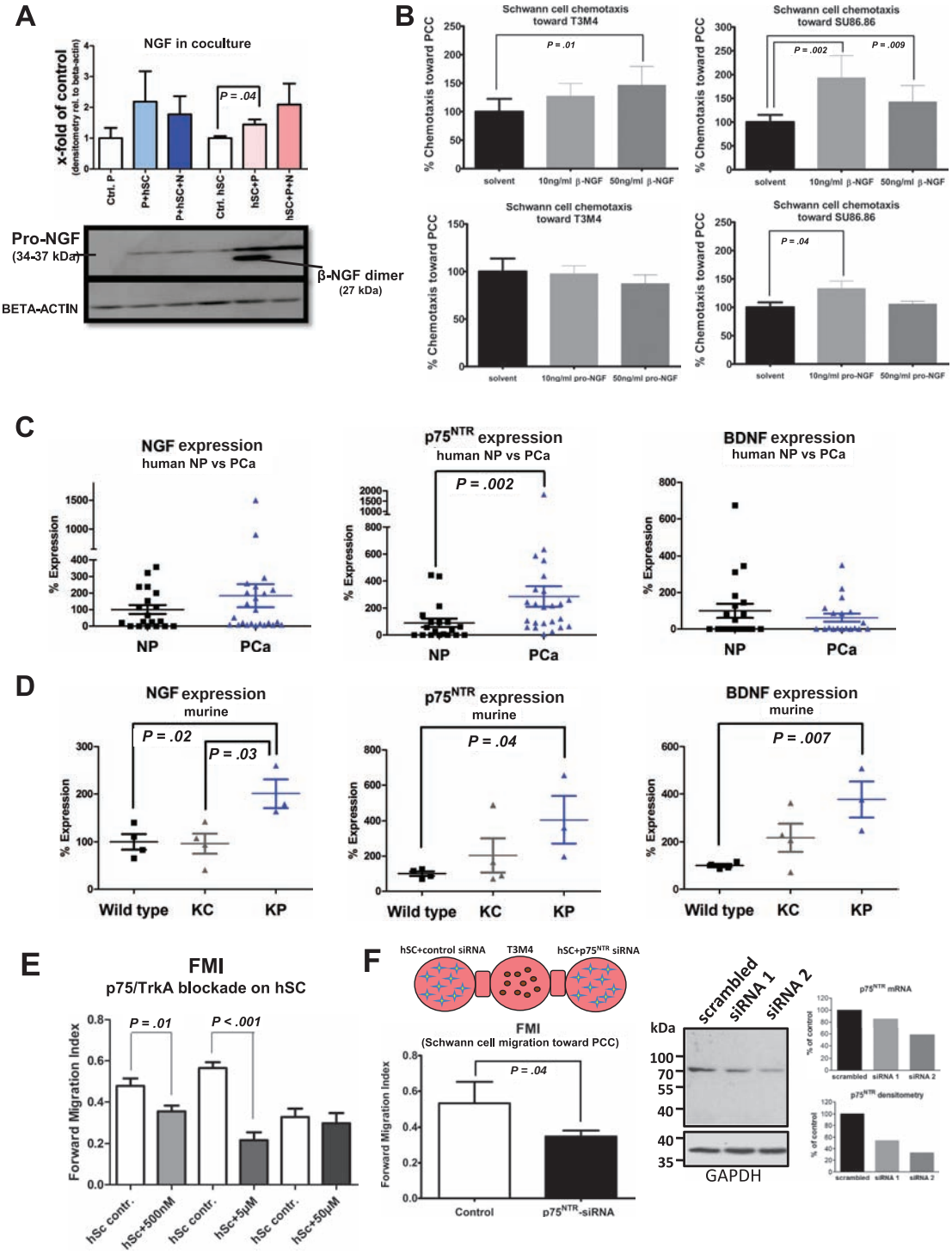

Figure 3. The impact of NGF-p75^{NTR} in Schwann cell carcinotropism. **A)** T3M4-pancreatic cancer cells were cocultured with either DRG neurons or with human Schwann cells (hSC, "P+hSC") or with both ("P+hSC+N"). Intracellular pro-NGF (NGF precursor) and mature beta-NGF dimer (mature beta-NGF monomer: 13.2 kDa) levels in pancreatic cancer cells and hSC were compared with mono-culture conditions ("Ctrl. P" for pancreatic cancer cell mono-culture, "Ctrl. hSC" for Schwann cell mono-culture). Unpaired t test. **B)** Human Schwann cells were placed into the upper compartment of a transwell (Boyden) chemotaxis assay supplied with increasing doses of beta-NGF (β-NGF, **upper row**) or pro-NGF (**lower row**) and quantified for their transmigration toward T3M4 or SU86.86 pancreatic cancer cells in the lower compartment. Mann-Whitney U test. **C)** QRT-PCR expression analysis of NGF, p75^{NTR}, and BDNF in normal human pancreas (NP) and pancreatic cancer (PCa) tissues. Mann-Whitney U test. **D)** QRT-PCR expression analysis of NGF, p75^{NTR}, and BDNF in wild-type (normal) pancreas, KC pancreas (containing PanIN precursor lesions), and KP pancreatic tumors. Unpaired t test. **E)** Human Schwann cells (hSC) were pretreated with the small molecule inhibitor Ro 08-2750 at a p75^{NTR}-inhibiting (at 500 nM and 5 μM) or both p75^{NTR}- and TrkA-inhibiting dose (50 μM), and their forward migration index (FMI) was compared to solvent-treated hSC ("hSc contr.") in the 3D migration assay. Mann-Whitney U test. **F)** The FMI of specific p75^{NTR}-siRNA-silenced human Schwann cells (hSC) and of control (scrambled) siRNA-transfected hSC that were confronted with T3M4 cells in the 3D migration assay. Silencing of p75^{NTR} via two different specific siRNA sequences (siRNA1 and siRNA2) was confirmed both at mRNA (via QRT-PCR) and protein level (via immunoblotting). Mann-Whitney U test. The results were created from three independent experiments. All statistical tests were two-sided.

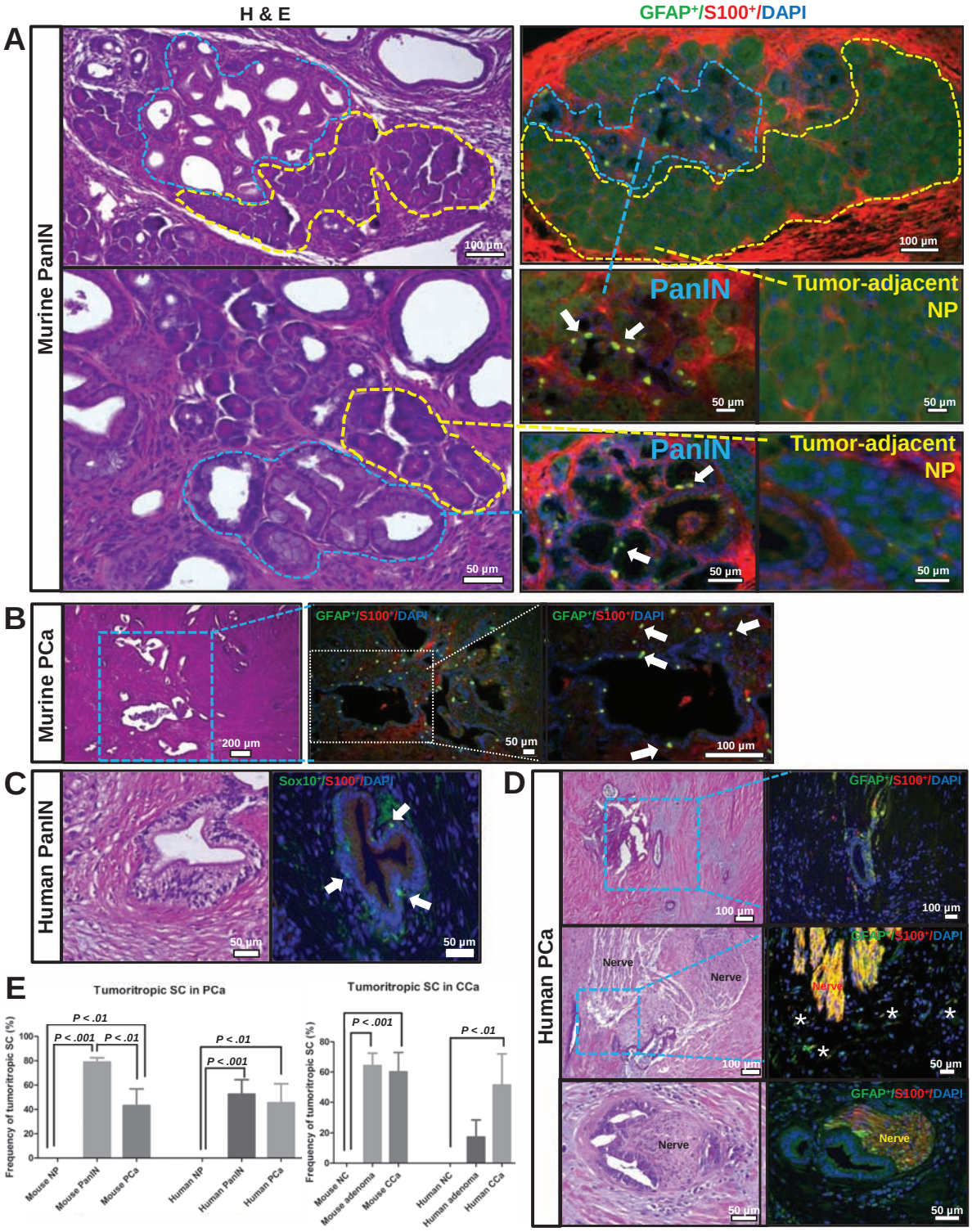

Figure 4. Emergence of Schwann cells around pancreatic cancer and colon cancer precursor lesions and cancer cell clusters. **A)** The pancreas in LSL-Kras^{G12D};p48-Cre (KC) mice is composed of areas containing pancreatic cancer precursor lesions (pancreatic intraepithelial neoplasia/PanIN, demarcated with **blue dashed lines** on the hematoxylin&eosin/H&E-stained image, **top left**) next to normal pancreatic parenchyma (**yellow dashed lines**). Immunolabeling of KC pancreas against the Schwann cell markers GFAP and S100 was performed to detect the specific presence of Schwann cells at the basolateral aspect of PanIN lesions (**white arrows**) as opposed to the tumor-adjacent normal parenchyma (the "on–off-phenomenon"). **B)** GFAP/S100 double-immunolabeled Schwann cells (**white arrows**) around cancer cell clusters in the LSL-Kras^{G12D};p48-Cre;Trp53$^{fl/fl}$ pancreatic cancer (PCa) model (KP mice). **C)** Human PanINs surrounded by S100-immunoreactive cells, which also contained the Schwann cell-identity marker Sox10. **D)** In human pancreatic cancer, cancer cell clusters (**upper panel**) were surrounded by nerve fibers, which were immunoreactive for GFAP/S100. GFAP/S100-double-immunoreactive cells (**asterisks**) were frequently observed not only within pancreatic nerves (**middle and lower panel**), but also outside them, in their direct neighborhood (**middle panel**). **E)** Frequency of Schwann cells around mouse and human PanIN, pancreatic cancer and colon cancer sites, and human colon adenomas. One-way analysis of variance with Bonferroni's posthoc analysis. The number of analyzed tissue samples was indicated in Supplementary Table 1 (available online).

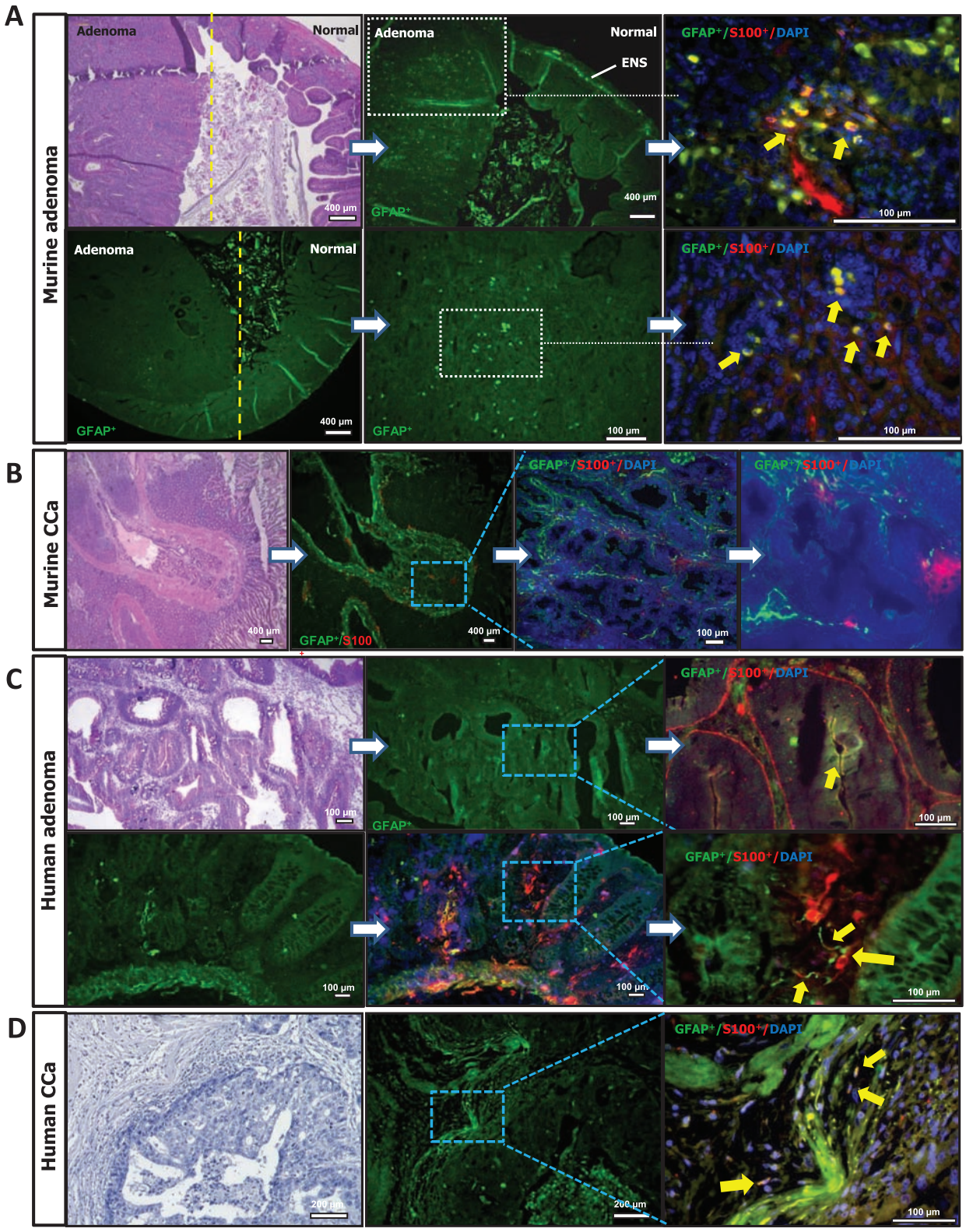

Figure 5. The occurence of Schwann cells in mouse and human colon adenomas and colon cancer. **A)** Mouse intestinal tissue (APC+/1638N model of intestinal adenomatosis) was double-immunolabeled against GFAP and S100, and the enrichment of particularly GFAP-immunoreactive cells in adenoma regions was compared to their specific presence in only the enteric nervous system (ENS) in neighboring normal intestinal regions (separated by the **yellow dashed line**). Note the portion of these cells that were double-immunoreactive for both GFAP and S100 (**yellow arrows, right upper panel**). **B)** Lack of GFAP/S100-double-immunoreactive Schwann cells around cancer cell clusters in the APC+/1638N;pVillin-Kras^{V12G} mouse colon cancer model. **C)** GFAP/S100-double-immunoreactive Schwann cells in human colon adenomas (**yellow arrows**). **D)** Detection and lower frequency of GFAP/S100-double-immunolabed Schwann cells around cancer cell clusters in human colon cancer tissues (**yellow arrows**) when compared with, eg, pancreatic cancer (also see Figure 3E). The number of analyzed tissue samples was indicated in Supplementary Table 1 (available online).

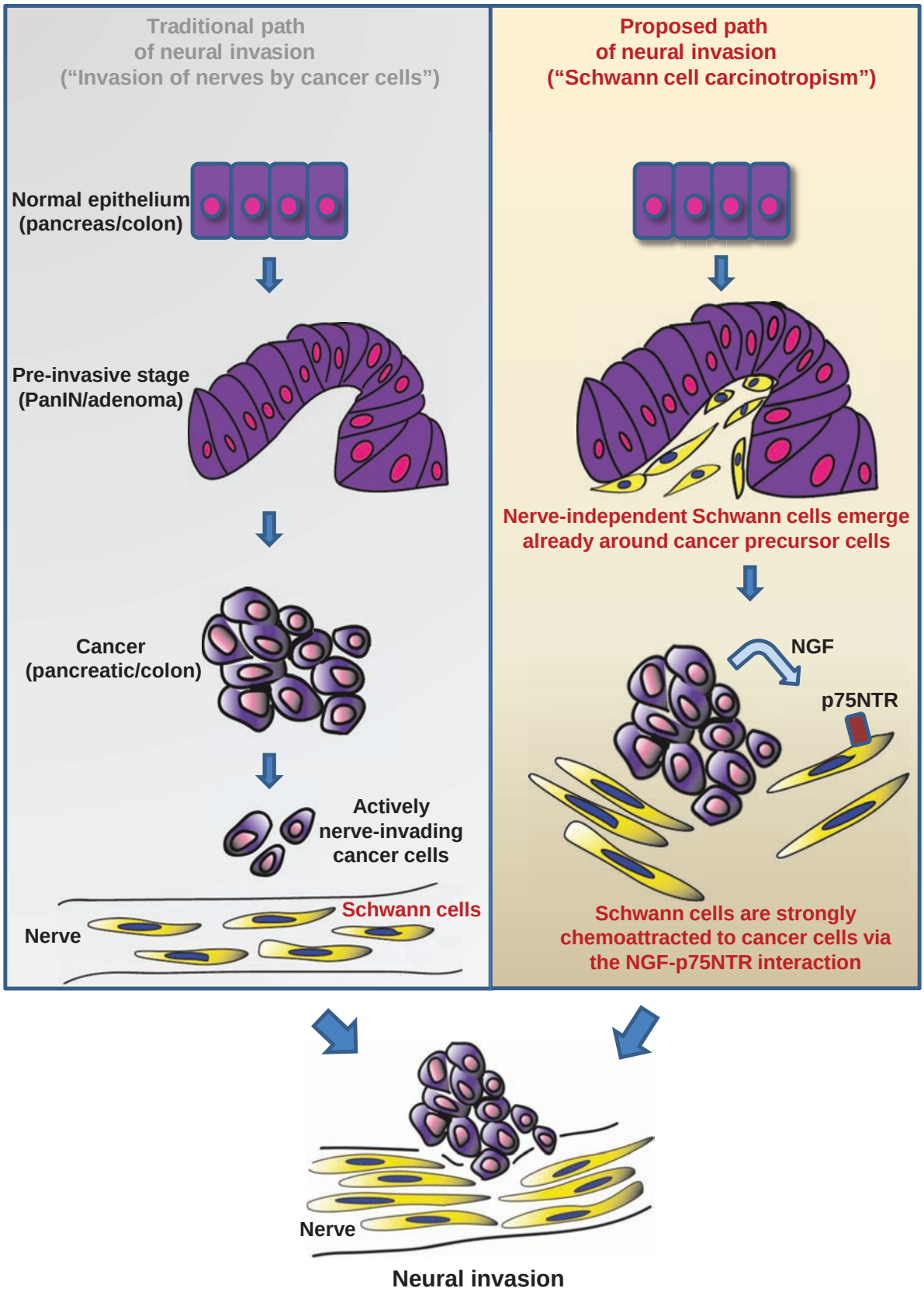

Figure 6. The proposed model for the potential generation of neural invasion in gastrointestinal cancers. The traditional model (**left panel**), which dictates that neural invasion results from the invasion of nerves by actively nerve-invading cancer cells that arise from their respective precursor lesions (ie, PanIN or colonic adenoma). The proposed model (**right panel**), which introduces the concept of "Schwann cell carcinotropism," ie, the chemoattraction of Schwann cells to cancer cells and their precursor lesions, paving the path for the generation of nerves around these early preneoplastic lesions.

and in human colon cancer specimens, Schwann cells were only occasionally detectable around adenomatous lesions or cancer cell clusters (Figure 5, C and D), as opposed to the unexceptional presence of Schwann cells around pancreatic neoplastic lesions.

Quantification of the frequency of Schwann cell associations with precursor (PanIN/ intestinal adenoma) or overt-cancer (pancreatic cancer/ CCa) lesions revealed that 78.9% (95% CI = 70.9 to 86.8%, $P < .001$, compared with normal tissue) of mouse and 52.5% (95% CI = 14.7 to 90.4%, $P < .001$) of human PanIN lesions, 43.2% (95% CI = –15.87 to 102.2%, $P < .01$) of ductular mouse pancreatic cancer cell clusters, and 45.4% (95% CI = –22.64 to 113.3%, $P < .01$) of human ductal pancreatic cancer sites exhibited close contact with Schwann cells (Figure 4E). Schwann cell-acinar cell associations were not detectable in murine or human NP. A similarly frequent association of Schwann cells with precursor or cancer cells was also observed around murine intestinal adenomatous clusters (mean of murine intestinal adenomas surrounded by Schwann cells = 64.2%, 95% CI = 28.6 to 99.8%, $P < .001$) and murine colon cancer cell clusters (mean of colon cancer cell clusters surrounded by Schwann cells = 60.1%, 95% CI = 4.5 to 115.7%, $P < .001$). In contrast, Schwann cells were encountered in merely 17.2% (95% CI = –126.9 to 161.4) of human colon adenomas and still in 51.4% (95% CI = –210.6 to 313.3%, $P < .01$) of colon cancer cell clusters (Figure 4E).

Discussion

In the present study, we demonstrate, on the one hand, that when pancreatic cancer cells are simultaneously confronted with neurons and Schwann cells of peripheral nerves, they migrate to neurons and not to glia cells. This observation underlines the preferential attraction of pancreatic cancer cells to neuronal components of peripheral nerves during NI. However, on the other hand, glia, ie, primary Schwann cells, launch a much earlier migration toward pancreatic cancer cells before these even start with their migration toward neurons. This Schwann cell migration is specific for malignant cells, absent against benign (non-neoplastic) cells and dependent upon NGF-TrkA-$p75^{NTR}$ signaling. Moreover, human and transgenic mouse pancreatic cancer tissues harbor abundant Schwann cells dispersed in tumor stroma and particularly around preneoplastic lesions.

Based on these observations, the differential cancer affinity of Schwann cells may reflect the dissimilarities in the divergent rate of NI in different cancers. Pancreatic cancer counts as one of the most neuro-affine GI tumors (1). Its near-100% NI rate surpasses that in more common GI tumors like colorectal cancer (1). In the present study, Schwann cells demonstrated a greater chemoattraction toward pancreatic cancer cells than colon cancer cells. Moreover, they lacked any affinity toward nonmalignant cells like HPDE, Mode-K, fibroblasts, or PaStC, with an intermediate affinity toward a CNS malignant cell (LN229). Hence, it can be assumed that malignant cells may represent more attractive targets for Schwann cells.

But how does cancer affinity fit into the biology of peripheral Schwann cells? Besides enwrapping single or multiple axons in peripheral nerves and facilitating signal transduction, Schwann cells play a key role in neural repair and regeneration. Following peripheral nerve injury, they can assume a reactive state and begin to dedifferentiate, to proliferate and mediate axon regeneration (27). An activated state of Schwann cells, eg, in pancreatic neuropathy, is possible in light of the previously reported intrapancreatic nerve damage in pancreatic cancer, which can be detected upon electron-microscopic analysis (28). Therefore, similar to their role in Wallerian degeneration and nerve regeneration, activated, carcinotropic Schwann cells are likely to serve as paths of axonal guidance toward cancer cells and result in "neurogenesis" around preneoplastic and neoplastic cells. This possibility is supported by the previously reported increased neural density and hypertrophy in pancreatic cancer tissues (2). This increased confrontation of cancer cells with $p75^{NTR}$-expressing and -upregulating carcinotropic Schwann cells and the accompanying axons may be the physical initiators of "neural invasion," not only in pancreatic but also other malignancies.

The lack of transgenic mouse models of pancreatic cancer with NI and pancreatic neuropathy (29) and the insufficient resolution of current in vivo time-lapse–imaging techniques (30) represent the major obstacles to verifying these novel observations in vivo in a functional manner. We demonstrated nerve-independent, stromally distributed Schwann cells in human pancreatic cancer and in two of the most commonly used transgenic mouse models of pancreatic cancer. Detection of Schwann cells in human and murine pancreatic cancer stroma may also certainly be due to the ongoing tissue remodeling in pancreatic cancer. However, this scattered Schwann cell population becomes more suspicious in terms of an in vivo migratory activity when one considers the near-absence of Schwann cells from intrapancreatic nerves in pancreatic cancer (15).

The current study concentrated on the NGF-TrkA-$p75^{NTR}$ signaling as a mediator of Schwann cell carcinotropism in two different gastrointestinal cancers. It is conceivable that further signaling pathways, eg, other neurotrophic factors or chemokines, may play a similar role in this particular chemoattraction. The source and the in-tissue path of the pancreatic and colonic Schwann cells that migrate toward cancer precursors still remain unknown. In addition to these aspects, a major objective for future studies should be to elucidate how cancer cells are affected and modulated by the Schwann cell chemoattraction they induce.

In summary, the current study demonstrated that Schwann cells are highly cancer-affine, and carcinotropic cells migrate toward cancer cells before these even start with invasion (Figure 6). The degree of tumor-tropic Schwann cell migration in part reflects the prevalence of NI in different gastrointestinal tumors and seems to be predominantly orchestrated by the action of NGF upon $p75^{NTR}$. These novel data urge us to revise and to even reverse our understanding of neural invasion in general, because, based on these results, it may be nerves—and not cancer cells—that first attack the other.

References

1. Liebig C, Ayala G, Wilks JA, et al. Perineural invasion in cancer: a review of the literature. *Cancer*. 2009;115(15):3379–3391.
2. Ceyhan GO, Bergmann F, Kadihasanoglu M, et al. Pancreatic neuropathy and neuropathic pain--a comprehensive pathomorphological study of 546 cases. *Gastroenterology*. 2009;136(1):177–186.
3. Reiser-Erkan C, Gaa J, Kleeff J. T1 pancreatic cancer with lymph node metastasis and perineural invasion of the celiac trunk. *Clin Gastroenterol Hepatol*. 2008;6(11):e41-e42.

4. Gil Z, Cavel O, Kelly K, et al. Paracrine regulation of pancreatic cancer cell invasion by peripheral nerves. *J Natl Cancer Inst*. 2010;102(2):107–118.
5. Bachem MG, Schneider E, Gross H, et al. Identification, culture, and characterization of pancreatic stellate cells in rats and humans. *Gastroenterology*. 1998;115(2):421–432.
6. Furukawa T, Duguid WP, Rosenberg L, et al. Long-term culture and immortalization of epithelial cells from normal adult human pancreatic ducts transfected by the E6E7 gene of human papilloma virus 16. *Am J Pathol*. 1996;148(6):1763–1770.
7. Ouyang H, Mou L, Luk C, et al. Immortal human pancreatic duct epithelial cell lines with near normal genotype and phenotype. *Am J Pathol*. 2000;157(5):1623–1631.
8. Vidal K, Grosjean I, evillard JP, et al. Immortalization of mouse intestinal epithelial cells by the SV40-large T gene. Phenotypic and immune characterization of the MODE-K cell line. *J Immunol Methods*. 1993;166(1):63–73.
9. Ceyhan GO, Demir IE, Altintas B, et al. Neural invasion in pancreatic cancer: a mutual tropism between neurons and cancer cells. *Biochem Biophys Res Commun*. 2008;374(3):442–447.
10. Hingorani SR, Wang L, Multani AS, et al. Trp53R172H and KrasG12D cooperate to promote chromosomal instability and widely metastatic pancreatic ductal adenocarcinoma in mice. *Cancer Cell*. 2005;7(5):469–483.
11. Lesina M, Kurkowski MU, Ludes K, et al. Stat3/Socs3 activation by IL-6 transsignaling promotes progression of pancreatic intraepithelial neoplasia and development of pancreatic cancer. *Cancer Cell*. 2011;19(4):456–469.
12. Jackson EL, Willis N, Mercer K, et al. Analysis of lung tumor initiation and progression using conditional expression of oncogenic K-ras. *Genes Dev*. 2001;15(24):3243–3248.
13. Nakhai H, Sel S, Favor J, et al. Ptf1a is essential for the differentiation of GABAergic and glycinergic amacrine cells and horizontal cells in the mouse retina. *Development*. 2007;134(6):1151–1160.
14. Jonkers J, Meuwissen R, van der Gulden H, et al. Synergistic tumor suppressor activity of BRCA2 and p53 in a conditional mouse model for breast cancer. *Nat Genet*. 2001;29(4):418–425.
15. Ceyhan GO, Demir IE, Rauch U, et al. Pancreatic neuropathy results in "neural remodeling" and altered pancreatic innervation in chronic pancreatitis and pancreatic cancer. *Am J Gastroenterol*. 2009;104(10):2555–2565.
16. Dai H, Li R, Wheeler T, et al. Enhanced survival in perineural invasion of pancreatic cancer: an in vitro approach. *Hum Pathol*. 2007;38(2):299–307.
17. Demir IE, Ceyhan GO, Liebl F, et al. Neural Invasion in Pancreatic Cancer: The Past, Present and Future. *Cancers*. 2010;2(3):1513–1527.
18. Ceyhan GO, Schafer KH, Kerscher AG, et al. Nerve growth factor and artemin are paracrine mediators of pancreatic neuropathy in pancreatic adenocarcinoma. *Ann Surg*. 2010;251(5):923–931.
19. Zhu Z, Friess H, diMola FF, et al. Nerve growth factor expression correlates with perineural invasion and pain in human pancreatic cancer. *J Clin Oncol*. 1999;17(8):2419–2428.
20. Pedraza CE, Podlesniy P, Vidal N, et al. Pro-NGF isolated from the human brain affected by Alzheimer's disease induces neuronal apoptosis mediated by p75NTR. *Am J Pathol*. 2005;166(2):533–543.
21. Finzsch M, Schreiner S, Kichko T, et al. Sox10 is required for Schwann cell identity and progression beyond the immature Schwann cell stage. *J Cell Biol*. 2010;189(4):701–712.
22. Hingorani SR, Petricoin EF, Maitra A, et al. Preinvasive and invasive ductal pancreatic cancer and its early detection in the mouse. *Cancer Cell*. 2003;4(6):437–450.
23. Kelly KA, Bardeesy N, Anbazhagan R, et al. Targeted nanoparticles for imaging incipient pancreatic ductal adenocarcinoma. *PLoS Med*. 2008;5(4):e85.
24. Cahoy JD, Emery B, Kaushal A, et al. A transcriptome database for astrocytes, neurons, and oligodendrocytes: a new resource for understanding brain development and function. *J Neurosci*. 2008;28(1):264–278.
25. Fodde R, Edelmann W, Yang K, et al. A targeted chain-termination mutation in the mouse Apc gene results in multiple intestinal tumors. *Proc Natl Acad Sci U S A*. 1994;91(19):8969–8973.
26. Janssen KP, Alberici P, Fsihi H, et al. APC and oncogenic KRAS are synergistic in enhancing Wnt signaling in intestinal tumor formation and progression. *Gastroenterology*. 2006;131(4):1096–1109.
27. Scholz J, Woolf CJ. The neuropathic pain triad: neurons, immune cells and glia. *Nat Neurosci*. 2007;10(11):1361–1368.
28. Bockman DE, Buchler M, Beger HG. Interaction of pancreatic ductal carcinoma with nerves leads to nerve damage. *Gastroenterology*. 1994;107(1):219–230.
29. Hruban RH, Adsay NV, Albores-Saavedra J, et al. Pathology of genetically engineered mouse models of pancreatic exocrine cancer: consensus report and recommendations. *Cancer Res*. 2006;66(1):95–106.
30. Eser S, Messer M, Eser P, et al. In vivo diagnosis of murine pancreatic intraepithelial neoplasia and early-stage pancreatic cancer by molecular imaging. *Proc Natl Acad Sci U S A*. 2011;108(24):9945–9950.
31. Ceyhan GO, Bergmann F, Kadihasanoglu M, et al. The neurotrophic factor artemin influences the extent of neural damage and growth in chronic pancreatitis. *Gut*. 2007;56(4):534–544.
32. Erkan M, Kleeff J, Gorbachevski A, et al. Periostin creates a tumor-supportive microenvironment in the pancreas by sustaining fibrogenic stellate cell activity. *Gastroenterology*. 2007;132(4):1447–1464.
33. Demir IE, Ceyhan GO, Rauch U, et al. The microenvironment in chronic pancreatitis and pancreatic cancer induces neuronal plasticity. *Neurogastroenterol Motil*. 2010;22(4):480–490, e112-e113.
34. Wang K, Demir IE, D'Haese JG, et al. The neurotrophic factor neurturin contributes toward an aggressive cancer cell phenotype, neuropathic pain and neuronal plasticity in pancreatic cancer. *Carcinogenesis*. 2014;35(1):103–113.

Funding

IED was supported by an institutional KKF stipend (B10-10) of the Faculty of Medicine of the Technische Universität München.

Notes

The study funder had no role in the design of the study, the collection, analysis, or interpretation of the data, the writing of the manuscript, nor the decision to submit the manuscript for publication. The authors declare no conflicts of interest. The results presented in the article are part of Ihsan Ekin Demir's PhD thesis and Alexandra Boldis' MD thesis.

Author contributions: IED, HF, HA, MeL, KPJ, and GOC designed the study. IED, AB, PLP, ST, EB, NK, TK, MaL, MM, and MeL performed the experiments. IED, AB, PLP, ST, EB, and NK analyzed the data. IED, AB, MeL, KPJ, HF, HA, and GOC wrote the manuscript. All authors critically read and agreed on the final version of the manuscript.

Affiliations of authors: Department of Surgery, Klinikum rechts der Isar, Technische Universität München, Munich, Germany (IED, AB, PLP, ST, EB, NK, TK, MM, MeL, KPJ, HF, GOC); Department of Internal Medicine II, Klinikum rechts der Isar, Technische Universität München, Munich, Germany (MaL, HA).